# The influence of black shale weathering on riverine barium isotopes

Quentin Charbonnier, Julien Bouchez, Jérôme Gaillardet, Damien Calmels, Mathieu Dellinger

Chemical Geology 594 (2022) 120741

Contents lists available at ScienceDirect

Chemical Geology

journal homepage: www.elsevier.com/locate/chemgeo

# The influence of black shale weathering on riverine barium isotopes

Quentin Charbonnier [a,b,*], Julien Bouchez [a], Jérôme Gaillardet [a,c], Damien Calmels [d], Mathieu Dellinger [e]

[a] Université de Paris, Institut de physique du globe de Paris, CNRS, F-75005 Paris, France
[b] Institute of Geochemistry and Petrology, Department of Earth Sciences, ETH Zurich, Clausiusstrasse 25, 8092 Zurich, Switzerland
[c] Institut Universitaire de France, Paris, France
[d] Université Paris-Saclay, CNRS, GEOPS, 91405, Orsay, France
[e] Environnements DYnamiques et TErritoires de la Montagne (EDYTEM), CNRS, Université Savoie Mont-Blanc, 73370 Le Bourget-Du-Lac, France

ARTICLE INFO

Editor: Dr Christian France-Lanord

*Keywords:*
Barium isotopes
Weathering
Black shales
Mackenzie Basin

ABSTRACT

Barium and its isotopes are receiving growing interest in their capacity to record the variation of the oceanic biological pump through geological timescales. Nonetheless, only little is known about the continental sources and processes that can drive the Ba flux and isotope composition to the ocean. Whereas the role of processes such as secondary phase formation, sorption and biological uptake on Ba isotopes has been recently investigated, the potential of various rock sources in producing a range of Ba isotope compositions remains poorly known. In particular, black shales often exhibit enrichment in Ba that might potentially be associated with various Ba isotope signatures.

In this study, we report the isotope composition of Ba in rivers with different relative contribution of black shale rocks in their catchments, located in the Mackenzie Basin (Northwest Canada). Both the dissolved and solid loads of the Mackenzie tributaries are enriched in heavy Ba isotopes with respect to the continental crust, which is consistent with an additional source to the weathering of igneous and siliciclastic rocks. Although the dissolved Ba abundance is partially driven by weathering processes, the river dissolved Ba isotope composition rather reflects a binary mixing between 1) a "classical" siliciclastic source (with a Ba isotope composition close to that of the upper continental crust $\delta^{138}$Ba $\sim 0.15 \pm 0.05$‰) and 2) an isotopically heavier source especially present in the Mackenzie Mountains (with a $\delta^{138}$Ba $\sim 0.40$‰). The positive relationships between dissolved $\delta^{138}$Ba and radiogenic osmium isotope ratios, as well as with sulphuric acid production, indicate that the heavy Ba source is tightly linked to the weathering of black shale. Although the exact reason for such heavy Ba isotope signatures remains elusive, this study emphasises the potential of black shale weathering in shifting the Ba isotope composition of the dissolved flux to the ocean towards heavier values.

## 1. Introduction

The study of barium (Ba) stable isotope fractionation at the Earth surface has recently gained momentum. The isotope composition of Ba ($\delta^{138}$Ba) in the ocean tracks barite precipitation in the water column (Horner et al., 2015; Cao et al., 2016; Bates et al., 2017; Bridgestock et al., 2018), a process that has been in turn suggested to be strongly linked to organic matter production, and thus to the oceanic biological $CO_2$ pump (Paytan and Griffith, 2007). As a result, Ba isotope signatures recorded in sedimentary archives are a possible tracer of the palaeo-biological productivity of the ocean (Bridgestock et al., 2019). However, continental sources and processes also potentially control the isotope composition of Ba in the ocean, and yet remain poorly constrained. Gong et al. (2019) have shown that chemical weathering, *i.e.* the dissolution of rock-forming minerals and the formation of secondary phases in soils, entails Ba isotope fractionation: light Ba isotopes are preferentially scavenged from the solutions, leaving soil and river waters enriched in heavy Ba isotopes. Beside Ba isotope fractionation occurring in soils, Ba isotopes can be fractionated by adsorption onto particles in rivers, as suggested by Gou et al. (2019), Bridgestock et al. (2021b) and Cao et al. (2021). In addition to these seemingly abiotic processes, biological uptake has been shown to significantly fractionate Ba isotope at the scales of soils (Bullen and Chadwick, 2016) and catchments (Charbonnier et al., 2020).

* Corresponding author at: Université de Paris, Institut de physique du globe de Paris, CNRS, F-75005 Paris, France
*E-mail address:* quentin.charbonnier@erdw.ethz.ch (Q. Charbonnier).

https://doi.org/10.1016/j.chemgeo.2022.120741
Received 25 August 2021; Received in revised form 16 January 2022; Accepted 25 January 2022
Available online 1 February 2022

Despite the large variety of processes that can produce Ba isotope variation in rivers, the data yet available for global rivers display limited range of dissolved Ba isotope composition (from 0.11 to 0.46‰; Hsieh and Henderson, 2017; Gou et al., 2019; Charbonnier et al., 2020; Cao et al., 2020, 2021; Bridgestock et al., 2021a). As this dataset remains very small ($N = 15$ rivers), it leaves open the question of the existence of other, potentially well-fractionated Ba sources to the ocean. In that respect, Tieman et al. (2020) report a wide variability of dissolved Ba isotope composition for brine waters associated with black shales, *i.e.* organic- and sulphide-rich, fine-grained, sedimentary rocks, with $\delta^{138}$Ba values ranging from −0.80 to +1.50‰. Additionally, black shales have been shown to display a strongly fractionated Ba isotope composition (1.19‰; N = 1; Tian et al., 2020) compared to other rocks (0.00 ± 0.04‰; N = 71; Nan et al., 2018). From these limited data, it can thus be hypothesized that continental regions underlain by black shales - and possibly other sedimentary rocks - might contribute with both light or heavy Ba isotope signature to the ocean. A significant influence of black shale weathering on riverine dissolved Ba fluxes is also supported by the observed positive relationships between dissolved Ba, sulphate ions, and the trace element rhenium (Re) in the Yamuna Basin rivers (Dalai et al., 2002a). Indeed, oxidative weathering of black shales tends to deliver appreciable amounts of dissolved sulphate and Re to rivers (Dalai et al., 2002b; Calmels et al., 2007; Horan et al., 2019), suggesting that a large fraction of river dissolved Ba on Earth could be delivered from the weathering of black shales.

In this study we explore the following hypothesis: black shale weathering results in large dissolved Ba fluxes to the ocean, with a Ba isotope composition that differs from that of the weathering of igneous and other siliciclastic rocks. A corollary of this hypothesis would be that past global variations in black shale weathering may have partially control the evolution of the oceanic Ba isotope composition. The Mackenzie river Basin (Canada) is a perfect natural laboratory to explore this hypothesis as weathering of black shale has been shown to have a salient impact on river chemistry in the Mackenzie Basin (Huh et al., 2004; Calmels et al., 2007; Horan et al., 2019). More specifically, a high dissolved Ba abundance has been reported for the Mackenzie River compared to other Arctic rivers (Guay and Falkner, 1998; Cooper et al., 2008) and to large rivers in general (Gaillardet et al., 2014). Such enrichment was attributed to the presence of specific rock sources, *e.g.* barite-rich sedimentary formations that could well be associated with black shales (Fraser and Hutchison, 2017), delivering dissolved Ba to the Mackenzie tributaries (Guay and Falkner, 1998).

To test for the role of black shale weathering on riverine Ba, we report new Ba isotope data on the dissolved load, suspended particulate matter, and river bed load of the main tributaries of the Mackenzie River. We use these data to discuss the sources of Ba in the Mackenzie Basin and show that there the weathering of black shales delivers a significant proportion of dissolved Ba with a heavy isotope composition.

## 2. Materials and methods

### 2.1. Geographical and geological setting

The Mackenzie Basin (Fig. 1), with a drainage area of $1.78 \times 10^6$ km$^2$, is one of the major Arctic river systems: the fourth largest in terms of water discharge (308 km$^3$/yr), second in terms of dissolved material flux, and first in terms of sediment discharge (Holmes et al., 2002; Millot et al., 2003). As the Mackenzie River drains northern latitudes, the average climate is cold (mean temperature of −4 °C).

Rainfall in the Mackenzie Basin is low and differs between the

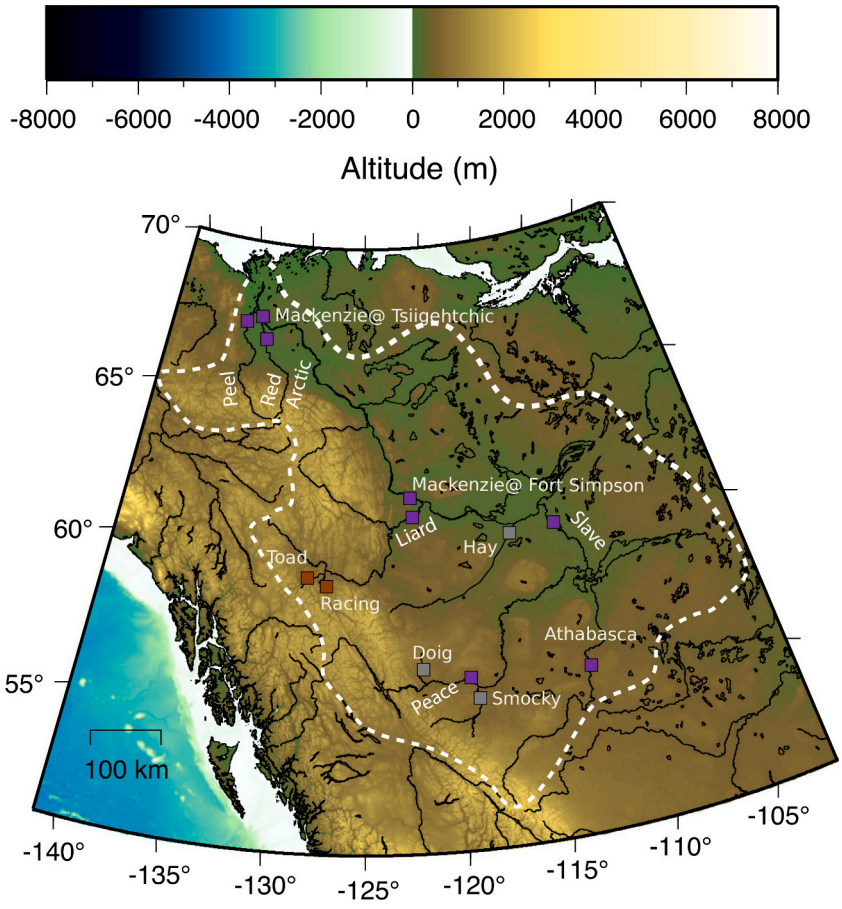


**Fig. 1.** Map of the Mackenzie Basin and location of the sampling sites, modified from Dellinger et al. (2014).

Mackenzie Mountains located in the western part of the basin (approximately 1000 to 1500 mm/yr) and the more arid lowlands located in the central and eastern parts (250 to 400 mm/yr) (Millot et al., 2003).

The Mackenzie Basin can be divided into three main geological units described in the following from West to East:

- **The North American Cordillera (Rocky mountains)** is the result of plate convergence at a tectonically active margin, where elevation ranges from 1000 to 2500 m. Most of the major tributaries of the Mackenzie River have their headwaters in this part of the basin. The dominant lithologies are Proterozoic to Mesozoic sedimentary rocks (carbonates, dolomites, shales, and black shales) (Reeder et al., 1972; Millot et al., 2003). The presence of carbonate and black shale, together with high erosion rates, results in weathering fluxes that are overwhelmed by carbonate weathering by sulphuric acid (Calmels et al., 2007) and petrogenic carbon oxidation (Horan et al., 2019), whereas silicate weathering is hampered by the cold climate (Millot et al., 2003). Igneous rocks are mostly present in the Western part of the Cordillera draining to the Pacific, for example drained by the Stikine and the Nass rivers (Gaillardet et al., 2003). Therefore, the contribution of igneous rock weathering to the Mackenzie river chemistry is limited. In this study, we report data from two rivers draining only the Cordillera: the Racing and the Toad rivers.
- **The Interior Platform** with a mean elevation of about 500 m, is underlain exclusively by sedimentary rocks such as shale, black shale, limestone, and evaporite. These rocks have Cambrian to Cretaceous ages (Millot et al., 2003). River solute fluxes are slightly more influenced by silicate weathering there than in the Rocky Mountains, likely because of 1) longer residence times of solid material in the weathering zone (due to lower erosion rates) and/or 2) production of dissolved organic matter in soils, which enhances silicate dissolution (Millot et al., 2003). Here we report and discuss data from three rivers draining only the Interior Platform: the Hay, Smocky, and Doig rivers.
- **The Canadian Shield** is an old craton dating from the Precambrian with a granitic to granodioritic chemical composition (Reeder et al., 1972; Gower et al., 1992; Millot et al., 2002, 2003). We do not report data from rivers draining the Canadian shield in the present study, as their overall contribution to the Mackenzie Basin dissolved load is low, and as their lithology is virtually free of sedimentary rocks (Gower et al., 1992; Millot et al., 2003).

The major tributaries of the Mackenzie Basin considered in the present study (Athabasca, Peace, Slave, Liard, Red Arctic and Peel) drain the Rocky Mountains and the Interior Platform, and join to form the main channel of the Mackenzie river.

In the Mackenzie Basin, river solute fluxes are strongly influenced by carbonate weathering (Millot et al., 2003). The main acid involved in rock weathering reactions differs between rivers, from a dominance of sulphuric acid for the rivers characterized by the highest erosion rates (*e.g.,* Red Arctic and Peel rivers) to a dominance of carbonic acid for the regions with the lowest erosion rates (*e.g.*, Slave and Peace rivers; Calmels et al., 2007).

### 2.2. Sampling and chemical composition of river water and sediments

The samples used in this study are from the Institut de physique du globe de Paris (IPGP) repository and have been collected during different sampling campaigns performed from 1996 to 2011 (Millot et al., 2003; Lemarchand and Gaillardet, 2006; Calmels et al., 2007; Millot et al., 2010; Tipper et al., 2012; Dellinger et al., 2014; Hilton et al., 2015). River waters were collected in acid-washed polypropylene containers and were filtered on site using Teflon filtration units (0.2−$\mu$m porosity). Water samples were acidified to pH ≈ 2 with ultra pure $HNO_3$ and placed in a cold room at 4 °*C*. Major anion and cation concentrations were measured using ion chromatography, dissolved silica concentrations by UV-VIS spectrophotometry, and trace elements by quadrupole ICP-MS (Inductively coupled plasma mass spectrometer) at IPGP.

River sediments were collected from the channel bottom to the surface along depth profiles, providing access to the whole spectrum of sediment grain size. Details about sampling procedures are given in Dellinger et al. (2014). Measurements for major and trace element concentration were carried out at the SARM (Service d'analyse des Roches et des Minéraux, INSU facility, Vandoeuvre-les-Nancy, France). Major element concentrations were measured using ICP-OES (Optical emission spectrometer), and trace element concentrations were measured using ICP-MS, with uncertainty typically around 10%.

### 2.3. Barium chemical separation and isotope measurements

The analytical procedure used for Ba separation is detailed in Charbonnier et al. (2020). Analyses were performed at the High-Resolution Analytical Platform PARI of IPGP. Before separation, the river water samples were evaporated to dryness and re-dissolved in 0.5 mL of 2.5 N HCl, while solid samples were digested in a $HNO_3$/HF mixture. Barium separation from its chemical matrix was perform by ion chromatography, using columns packed with the cation resin AG50-X8. In this protocol, the matrix is eluted using 13 mL of 2.5 N HCl, following which Ba is eluted in 15 mL of 6 N HCl. Eluate purity as well as yields were evaluated by quadrupole ICP-MS to ensure a total recovery and proper purification of Ba from the sample (recovery and purification results are presented in Table S1). The total procedure blank was lower than 0.2 ng of Ba, for a minimum of 400 ng for each sample. The isotope ratios of Ba were measured by MC-ICP-MS (Multi-collector ICP-MS Neptune, Thermo Fisher Scientific) using a quartz, double spray chamber as an introduction system. All concentrations of standard and sample solutions were adjusted to 100 $\mu g/L$. The instrumental mass fractionation was corrected for using the sample-standard bracketing method. Mass dependent fractionation was checked by plotting the $^{137}Ba/^{135}Ba$ *vs.* $^{137}Ba/^{134}Ba$ ratios (see Charbonnier et al., 2020). The isotope ratios of Ba are reported as $\delta^{13x}Ba$:

$$\delta^{13x}Ba_{smp}\left(‰\right) = \left(\frac{^{13x}Ba/^{134}Ba_{smp}}{^{13x}Ba/^{134}Ba_{std}} - 1\right) \times 1000 \quad (1)$$

with $x = 7$ or 8, *smp* the sample isotope ratios and *std* the standard isotope ratios (NIST SRM3104a). We do not use directly the $^{138}Ba$ signal because of the presence of Ce and La in the chromatography eluates of sediment samples, and thus only rely on $^{137}Ba/^{134}Ba$ ratios. However, for the sake of consistency with the literature data, we converted our data to $\delta^{138}Ba$ using the mass-dependent relationship: $\delta^{138}Ba \approx 1.33 \times \delta^{137}Ba$.

Uncertainties on $\delta^{138}Ba$ values are reported as 95%-confidence intervals, calculated as follows:

$$CI95\% = t_{n-1} \times \frac{S.D.}{\sqrt{n}} \quad (2)$$

with *S. D.* the standard deviation over the *n* measurements of the sample (typically $n = 3$), and $t_{n-1}$ the Student's law factor with *n*-1 degrees of freedom, at 95%-confidence level.

The long-term reproducibility and accuracy (over one year and a half) of the measurements were checked using our separation protocol on the reference materials JB-2 (−0.02 ± 0.14‰ 2 S.D.; 0.17 CI 95%; $N = 3$), BaBe27 (−0.80 ± 0.18‰ 2 S.D.; 0.04 CI 95%; $N = 18$), BCR-2 (0.05 ± 0.08‰ 2 S.D.; 0.04 CI 95%; $N = 6$) and AGV-2 (0.05 ± 0.12‰ 2 S.D.; 0.05 CI 95% $N = 8$), matching well the values reported by Van Zuilen et al. (2016) and Charbonnier et al. (2018).

## 3. Results

The data for river dissolved and particulate loads in the Mackenzie Basin are reported in Tables 1 and 2, respectively.

### 3.1. River dissolved Ba abundance and isotope composition

The dissolved Ba concentration in the Mackenzie Basin ranges from 0.20 to 0.56 $\mu$mol/L, which is significantly higher than for other large rivers (between 0.07 and 0.20 $\mu$mol/L on average; Guay and Falkner, 1998; Gaillardet et al., 2014; Cao et al., 2016), except for the Huanghe Basin (Gou et al., 2019). In the following, we do not perform any correction for rain inputs on dissolved Ba concentrations, and consider raw dissolved Ba concentrations as being representative of water-rock interactions. Indeed, the abundance of Ba in sea water is low with respect to that generally observed in rivers (Dehairs et al., 1980), making the contribution of sea salt to river dissolved Ba likely negligible. As a matter of fact, even assuming that the entirety of the dissolved chlorine in the rivers of the Mackenzie derives from sea salt, the contribution of Ba from the rain water contribution is less than 1% across our dataset.

As dissolved Ba concentrations in the Mackenzie rivers might be influenced by dilution depending on the amount of available water (Cooper et al., 2008), we normalise dissolved Ba concentration by that of a soluble element, here sodium (Na), corrected from sea-salt and halite dissolution (hereafter called *Na**; Millot et al., 2003). The Rocky tributaries are enriched in Ba (with respect to Na), whereas Interior Platform tributaries are characterized by the lowest $(Ba/Na^*)_{diss}$ ratios and the Mackenzie main tributaries show intermediate values (Table 1).

The isotope composition of dissolved Ba in the Mackenzie Basin ranges from 0.13‰ to 0.61‰ (Table 1), which is higher than most values reported hitherto for other rivers (Hsieh and Henderson, 2017; Gou et al., 2019; Cao et al., 2020; Charbonnier et al., 2020; Bridgestock et al. 2021a, 2021b). Like for the Ba/Na ratio, the $\delta^{138}$Ba values of the Mackenzie dissolved load displays a gradient with high values for Rocky tributaries, lowest values for Interior Platform tributaries and intermediate values for Mackenzie main tributaries.

### 3.2. River solid Ba abundance and isotope composition

Mackenzie river sediments display a strong enrichment in Ba compared to the Upper Continental Crust (UCC), with Ba concentrations ranging from 455 to 1542 mg/kg (against around 600 mg/kg for the UCC; Rudnick and Gao, 2003). As for the dissolved load, Ba abundance in river sediments can directly be interpreted without taking into account carbonate or evaporite, since Ba is not significantly hosted by these mineral types (Gou et al., 2019; Charbonnier et al., 2020). The ratio Ba/Al of river sediments (Al being an insoluble element used to correct for potential "dilution" effects of Ba concentration by Ba-free material such as quartz or organic matter) ranges from 0.01 to 0.045 (in ppm/ppm ratio). This corresponds to a two- to five-fold enrichment relative to the UCC ($(Ba/Al)_{UCC} \sim 0.007$; Rudnick and Gao, 2003). This significant enrichment in Ba is accompanied with an overall heavier Ba isotope composition ($\delta^{138}Ba_{sed}$ values ranging from −0.02 to 0.35‰), compared to the UCC ($\delta^{138}Ba_{UCC} \approx 0.00$‰; Nan et al., 2018). The $\delta^{138}$Ba values of the suspended particulate matter do not show any correlation with the Al/Si ratio (not shown), commonly used as a tracer of sediment grain size (Bouchez et al., 2011).

### 3.3. The partitioning of Ba and its isotopes amongst the river dissolved and solid loads

Quantification of how Ba and its isotopes are partitioned between the various compartments of the river load (dissolved matter, suspended matter, and bed sands) is informative to identify source and process controls on river Ba fluxes (*e.g.*, Dellinger et al., 2021 for rhenium

**Table 1**
Dissolved major and trace element concentrations, Ba isotope compositions and Sr-Os isotope ratios of the Mackenzie Basin. All concentrations are in µmol/L

| Sample | Date | Latitude (N) | Longitude (W) | River | Unit | $Na^+$ | $K^+$ | $Mg^{2+}$ | $Ca^{2+}$ | $HCO_3^-$ | $Cl^-$ | $SO_4^{2-}$ | $Ba^{2+}$ | $^{187}Os/^{188}Os$ | $^{87}Sr/^{86}Sr$ | $\delta^{138}$Ba | Uncertainty (IC95%) |
|---|---|---|---|---|---|---|---|---|---|---|---|---|---|---|---|---|---|
| CAN09–51 | 22-7-2009 | 67.429 | 133.782 | Red Arctic | | 150 | 22 | 566 | 1147 | 1568 | 16 | 857 | 0.27 | 2.00 | 0.713 | 0.43 | 0.10 |
| CAN09–03 | 15-7-2009 | 61.837 | 121.285 | Liard | | 83 | 15 | 378 | 877 | 1686 | 10 | 338 | 0.29 | 2.37 | 0.715 | 0.42 | 0.05 |
| CAN09–20 | 20-7-2009 | 61.889 | 121.388 | Mackenzie at Fort Simpson | | 315 | 22 | 262 | 682 | 1432 | 208 | 233 | 0.24 | | | 0.35 | 0.07 |
| CAN09–43 | 22-7-2009 | 67.458 | 133.723 | Mackenzie at Tsiigetchic | | 249 | 20 | 367 | 833 | 1564 | 190 | 373 | 0.33 | 1.89 | 0.711 | 0.34 | 0.15 |
| CAN96–15 | 22-8-1996 | | | Peace | Main tributaries | 78 | 12 | 267 | 713 | 1766 | 12 | 142 | 0.33 | 1.79 | 0.713 | 0.13 | 0.01 |
| CAN09–28 | 18-7-2009 | 60.016 | 111.890 | Slave | | 300 | 23 | 313 | 798 | 1741 | 168 | 271 | 0.38 | | 0.711 | 0.32 | 0.10 |
| CAN09–37 | 21-7-2009 | 67.332 | 134.868 | Peel | | 173 | 14 | 624 | 1124 | 2173 | 59 | 661 | 0.40 | 1.70 | 0.716 | 0.44 | 0.09 |
| CAN96–5 | 15-8-1996 | | | Peel | | 167 | 13 | 673 | 1142 | 2381 | 37 | 761 | 0.45 | 1.70 | 0.716 | 0.33 | 0.03 |
| CAN96–42 | 31-8-1996 | | | Athabasca | | 324 | 34 | 322 | 734 | 2046 | 34 | 209 | 0.36 | 2.25 | 0.710 | 0.27 | 0.03 |
| CAN99–71 | | | | Doig | Interior | 222 | 24 | 160 | 384 | 241 | 6 | 422 | 0.20 | | 0.710 | 0.14 | 0.07 |
| CAN96–16 | | | | Smoky | platform | 233 | 22 | 323 | 815 | 2110 | 27 | 225 | 0.47 | | 0.710 | 0.29 | 0.07 |
| CAN96–33 | | | | Hay | | 442 | 33 | 381 | 844 | 1846 | 44 | 483 | 0.22 | 1.63 | 0.711 | 0.23 | 0.09 |
| CAN96–19 | | | | Racing | Rocky | 30 | 14 | 589 | 842 | 2047 | 10 | 477 | 0.56 | 3.86 | 0.731 | 0.61 | 0.09 |
| CAN96–20 | | | | Toad | Mountains | 42 | 10 | 635 | 1014 | 2030 | 8 | 710 | 0.24 | 2.38 | 0.734 | 0.57 | 0.12 |

Major element concentrations and radiogenic Sr ratios are from Millot et al. (2003).
Radiogenic Os ratios are from Huh et al. (2004).
Information about CAN96 and CAN99 samples can be found in Millot et al. (2003).

**Table 2**
Chemical and Ba isotope data of solid load of the Mackenzie Basin.

| Sample | Date | Latitude (N) | Longitude (W) | River | Sample | [spm] mg/L | Al | Ba | Al/Si | $\delta^{138}$Ba | Uncertainty (IC95%) | $\delta^{7}$Li | Li |
|---|---|---|---|---|---|---|---|---|---|---|---|---|---|
| CAN09_49 | 22-7-2009 | 67.429 | 133.782 | Red Arctic | Bank material | | 43,372 | 977 | 0.15 | 0.26 | 0.07 | 0.27 | 37 |
| CAN09_51 | 22-7-2009 | 67.429 | 133.782 | Red Arctic | Suspended sed. | 417 | 79,022 | 1125 | 0.31 | 0.35 | 0.07 | −2.41 | 78 |
| CAN09_02 | 15-7-2009 | 61.838 | 121.284 | Liard | Suspended sed. | 191 | 63,896 | 873 | 0.23 | 0.05 | 0.19 | −1.10 | 49 |
| CAN09_11 | 16-7-2009 | 61.842 | 121.296 | Liard | Bank material-(sandbar) | | 28,744 | 688 | 0.08 | 0.00 | 0.18 | 4.01 | 16 |
| CAN10_49 | 13-9-2010 | 61.823 | 121.298 | Liard | Suspended sed. | 79 | 73,830 | 954 | 0.28 | 0.23 | 0.16 | | 64 |
| CAN09_54 | 22-7-2009 | 67.454 | 133.707 | Mackenzie | Bank material | | 40,244 | 796 | 0.13 | 0.28 | 0.08 | 0.79 | 27 |
| CAN09_47 | 22-7-2009 | 67.458 | 133.723 | Mackenzie | Suspended sed. | 505 | 76,477 | 924 | 0.30 | 0.28 | 0.20 | −1.66 | 68 |
| CAN10_32 | 9-9-2010 | 68.409 | 134.080 | Mackenzie | Suspended sed. | 162 | 90,608 | 940 | 0.38 | 0.13 | 0.02 | −1.69 | 79 |
| CAN10_38 | 9-9-2010 | | | Mackenzie | Bedload | | 32,258 | 687 | 0.10 | 0.14 | 0.02 | | 21 |
| CAN09_38 | 21-7-2009 | 67.332 | 134.869 | Peel | Suspended sed. | 150 | 72,364 | 1086 | 0.26 | 0.22 | 0.05 | −2.24 | 71 |
| CAN09_40 | 21-7-2009 | 67.332 | 134.869 | Peel | Suspended sed. | 113 | 80,981 | 1190 | 0.30 | 0.06 | 0.11 | −2.06 | 82 |
| CAN09_41 | 21-7-2009 | 67.332 | 134.869 | Peel | Bedload | | 40,620 | 1233 | 0.12 | 0.35 | 0.16 | −0.32 | 34 |
| CAN10_04 | 7-9-2010 | 67.330 | 134.865 | Peel | Suspended sed. | 121 | 72,401 | 1190 | 0.26 | −0.02 | 0.12 | −2.53 | 69 |
| CAN10_07 | 7-9-2010 | 67.330 | 134.865 | Peel | Bedload | | 34,205 | 1542 | 0.09 | 0.25 | 0.08 | 0.09 | 28 |
| CAN99_60 | | | | Toad | Suspended sed. | 365 | 71,206 | 818 | 0.30 | 0.20 | 0.07 | | |
| CAN99_60 | | | | Toad | Bedload | | 50,284 | 559 | 0.21 | 0.26 | 0.12 | | |
| CAN99_64 | | | | Racing | Bedload | | 41,188 | 455 | 0.15 | 0.28 | 0.08 | | |

Al, Si, Li abundances and Li isotopes are from Dellinger et al. (2014).
All abundances are in mg/kg.

fluxes). First, this examination can be performed on a flux basis, where the partitioning of Ba between the dissolved and solid loads is calculated as follows:

$$w^{Ba} = \frac{[Ba]_{diss}}{[Ba]_{diss} + [Ba]_{spm} \times [spm]} \quad (3)$$

with $[Ba]_{diss}$ the dissolved concentration of Ba in $\mu$g/L, $[Ba]_{spm}$ the Ba concentration in river suspended sediments in mg/kg, and [*spm*] the long-term suspended particulate matter concentration in g/L (Carson et al., 1998). The fraction of riverine Ba that is transported as dissolved species ranges from 2% for the Red Arctic river, to 23% for the Racing river. On average, dissolved Ba represents only 14% of the total Ba. These numbers suggest that in the Mackenzie Basin the riverine Ba export is dominated by the transport of unweathered, Ba-bearing minerals, or of Ba-bearing secondary weathering solid phases.

Second, the partitioning can also be examined using elemental and isotope ratios. In the Mackenzie Basin, dissolved Ba/Na ratios are systematically lower than their solid counterparts, be they suspended matter or bed sands (Fig. 2a). Again, this comparison suggests that a minor fraction of Ba is mobilised through rock dissolution during weathering in the Mackenzie Basin, and/or that processes scavenge dissolved Ba, as previously suggested (Gong et al., 2019; Gou et al.,

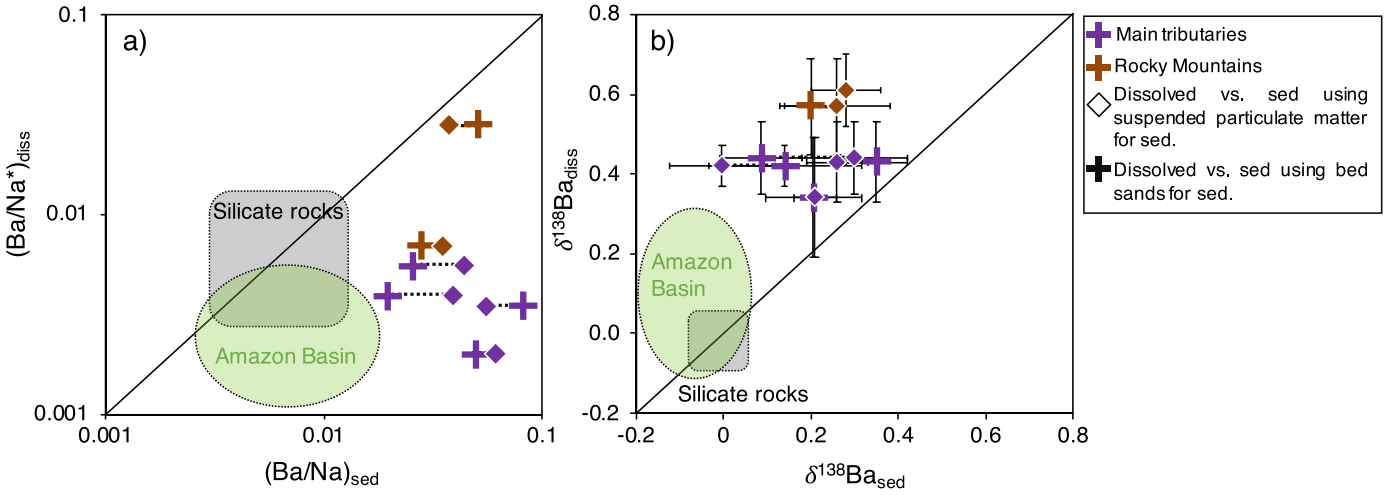


**Fig. 2.** Comparison between river dissolved, suspended particulate matter, and bed sands a) Ba/Na ratios and b) $\delta^{138}$Ba signatures. Amazon Basin data from Charbonnier et al. (2020) and silicate rock data from Taylor and McLennan (1995), Rudnick and Gao (2003) and Nan et al. (2018) have been added for comparison.

2019; Charbonnier et al., 2020; Bridgestock et al., 2021b). The dissolved $\delta^{138}$Ba is significantly heavier than those of the river suspended and bed sediments (Fig. 2b).

## 4. Discussion

As explained above, distinct Ba/Na ratios and $\delta^{138}$Ba between the dissolved and solid loads suggest that during weathering in the Mackenzie Basin some processes affect Ba and fractionate its isotopes. Nevertheless, the overall heavy $\delta^{138}$Ba signatures in both the dissolved and solid loads - compared to other river systems and to most rocks analyzed hitherto ($\delta^{138}$Ba = 0.00 ± 0.04‰; Nan et al., 2018)- also suggest the role of additional heavy $\delta^{138}$Ba sources. In the following discussion, we first investigate whether or not the observed heavy dissolved Ba isotope compositions derive from the presence of specific river Ba sources in the Mackenzie, rather than from processes fractionating Ba isotopes during weathering. Then we determine the nature of these potential additional sources.

### 4.1. A high-$\delta^{138}$Ba lithological component in the Mackenzie basin bedrock inferred by river sediments

The overall low silicate weathering rates in the Mackenzie Basin suggests that the composition of the silicates in river sediments are mostly controlled by provenance rather than modern weathering processes (Millot et al., 2003; Dellinger et al., 2014). Below, we use the elemental and isotope composition of river sediments to constrain the Ba isotope composition of potential sources of river Ba in the Mackenzie Basin.

Shale erosion and subsequent weathering are likely to be a significant contributor to the Ba river budget of the Mackenzie. Indeed, lithium (Li) and its isotopes in river sediments reveal the significant contribution of fine-grained meta-sedimentary formations (*i.e.* shales) to the river solid loads across the Mackenzie Basin (Dellinger et al., 2014). In Fig. 3a, b, we report the Ba isotope composition of river sediments against their Li/Al ratio and Li isotope composition ($\delta^7$Li; Fig. 3). These mixing diagrams suggest that Mackenzie river sediments can be interpreted as derived from a mixture between (1) a component of relatively low Li/Al ratio and high $\delta^7$Li with an UCC-like $\delta^{138}$Ba (0.00‰; Nan et al., 2018; grey rectangle in Fig. 3a,b), that can be attributed to the erosion of igneous rocks; and (2) a component characterized by higher Li/Al ratio and lower $\delta^7$Li values, that is typical of shale material (Dellinger et al., 2014, brown and yellow rectangles in Fig. 3a,b). This observation is consistent with the prominent erosion of fine-grained sedimentary rocks, driving the Ba abundance and isotope composition of river sediments in the Mackenzie Basin.

Fig. 3c shows that Mackenzie river sediments are enriched in Ba compared to shale and igneous rocks that are thought to have similar Ba/Al ratios (Taylor and McLennan, 1995; Rudnick and Gao, 2003), suggesting that a specific rock component, enriched in heavy Ba isotopes, is needed to explain the overall high Ba abundance observed in our sediment dataset.

We note that suspended sediments are less enriched in Ba than river bed sands, with $(Ba/Al)_{spm}/(Ba/Al)_{rbs}$ ratios between 0.4 and 0.6 (Fig. 3d,e). Given the low weathering intensity experienced by river sediments in the Mackenzie Basin (Millot et al., 2003; Dellinger et al., 2014) such Ba depletion in fine sediments is unlikely to derive from chemical weathering. Suspended sediments that are the most Ba-

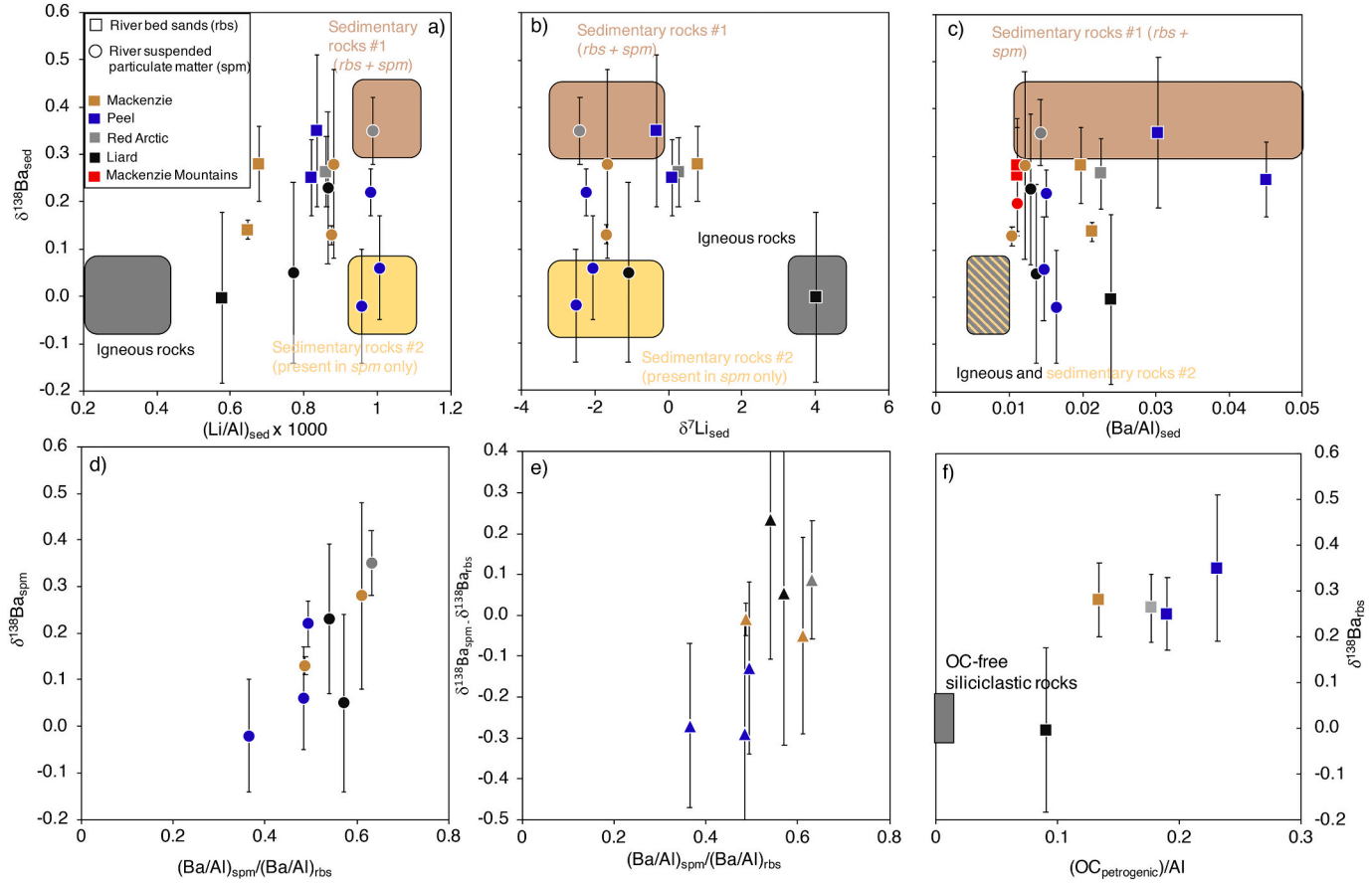


**Fig. 3.** River sediment $\delta^{138}$Ba (*rbs* = river bed sediments, *spm* = suspended particulate matter) values *vs.* (a) Li/Al ratios; (b) $\delta^7$Li values; (c) Ba/Al ratios; *vs.* (d) $(Ba/Al)_{spm}/(Ba/Al)_{rbs}$; (e) $\delta^{138}Ba_{spm} - \delta^{138}Ba_{rbs}$ *vs.* $(Ba/Al)_{spm}/(Ba/Al)_{rbs}$; and (f) $\delta^{138}Ba_{rbs}$ *vs.* Petrogenic organic carbon ($OC_{petrogenic}$)/Al. $OC_{petrogenic}$ data are from Hilton et al. (2015).

depleted compared to the corresponding river bed sands are also characterized by the lightest Ba isotope composition (Fig. 3d,e), close to that of siliciclastic rocks (Nan et al., 2018). We thus propose that this relatively low-Ba end member represents the fine phase eroded from sedimentary rocks such as "recycled" clays (Dellinger et al., 2014). This fine component would not be present in appreciable amount in river bed sands, but would be characterized by high Li/Al ratios and low $\delta^7$Li values (Fig. 3a,b).

The Ba-richest samples, which also tend to display the heaviest Ba isotope composition (Fig. 3c), are from rivers hosting a significant proportion of black shale in their drainage basin, such as the Peel or Red Arctic (Millot et al., 2003; Huh et al., 2004). Recent studies reveal that black shales are characterized by a wide range of Ba isotope signatures, although the exact reason for such broad range of Ba isotope variations remains unclear (Tian et al., 2020; Tieman et al., 2020). As black shales contain significant amounts of petrogenic organic carbon (*e.g.*, Hilton et al., 2015; Horan et al., 2019), we can test for the role of black shale erosion in driving the Ba isotope composition of Mackenzie river sediments by examining the relationship between river bed sediment $\delta^{138}$Ba *vs.* the abundance of petrogenic-derived particulate organic carbon over Al ratio ($OC_{petrogenic}$/Al; Fig. 3f) (data from Hilton et al., 2015). In this particular analysis, we do not use river suspended sediments as the contribution of petrogenic organic carbon (obtained from radiocarbon) tends to be overestimated in fine-grained sediments in the Mackenzie River because of the presence of pre-aged biospheric organic carbon, while bed sediments are almost free of biogenic organic carbon (Hilton et al., 2015). The $\delta^{138}$Ba values of river bed sediments show a broad positive relationship with their $OC_{petrogenic}$/Al ratios. The relationship of Fig. 3f shows that the heavy Ba isotope signatures observed in some of the river sediments of the Mackenzie Basin are typically associated with high contents of petrogenic organic carbon, hinting at a possible role of black shale erosion in setting river Ba isotope composition there.

From this array of evidence, we contend that in the Mackenzie river basin, black shale might play a role in setting the wide range of observed Ba isotope composition of river sediment. By construction, the presence of rocks with a particularly high $\delta^{138}$Ba should also drive the resulting dissolved $\delta^{138}$Ba. We test for this hypothesis below.

### 4.2. Source vs. process controls on river Ba dissolved abundance

Variations in river dissolved chemistry are controlled by the mixing of different sources (*e.g.,* silicate *vs.* carbonate rock weathering; Gaillardet et al., 1999), and/or various Earth surface processes (*e.g.,* formation of secondary phases such as clays or oxides, adsorption onto mineral or organic surfaces, biological uptake; Bullen and Chadwick, 2016; Gong et al., 2019; Gou et al., 2019). In the following section, we assess the relative role of different sources and processes in setting dissolved Ba isotope signatures in rivers of the Mackenzie Basin.

#### 4.2.1. A minor role of secondary processes in driving river Ba isotope composition variability across the Mackenzie Basin

The positive relationship between $\delta^{138}Ba_{diss}$ values and $Ba/Na^*_{diss}$ (Fig. 4) in the Mackenzie Basin indicates that the strongest dissolved Ba enrichment is related to a heavy Ba isotope composition. This trend can be interpreted as either the mixture of two different Ba sources, or a process which preferentially scavenges the heavy isotopes of Ba from soil solutions or from river waters.

Previous studies have addressed the influence of secondary processes on Ba isotopes, such as clay or oxide (Gong et al., 2019), biological uptake (Bullen and Chadwick, 2016; Charbonnier et al., 2020), and sorption onto river particles (Coffey et al., 1997; Samanta and Dalai, 2016; Gou et al., 2019; Bridgestock et al., 2021b). Generally speaking, all the aforementioned secondary processes are known to leave a residual dissolved Ba component that is enriched in heavy Ba isotopes. Considering that Na is a conservative element (meaning not significantly incorporated into secondary solids, sorbed onto particles, nor taken up by the biota), in this scenario an inverse relationship would be expected between $Ba/Na^*_{diss}$ ratios and $\delta^{138}Ba_{diss}$ values. An opposite trend is observed (Fig. 4), indicating that these processes cannot be the main drivers of $\delta^{138}Ba_{diss}$ variations at the scale of the Mackenzie River system.

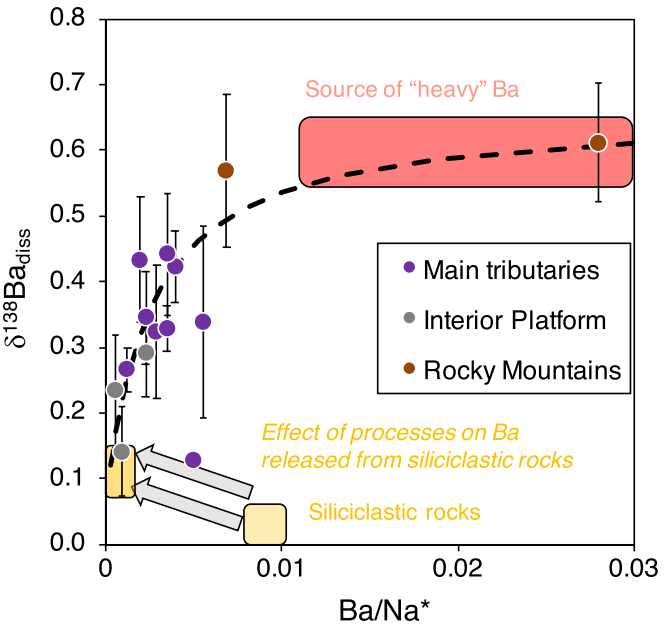


**Fig. 4.** Dissolved $\delta^{138}$Ba values *vs.* Ba/Na* molar ratios in the Mackenzie Basin ("*" refers to the dissolved Na river content corrected for rain inputs). The stippled curve corresponds to a mixing hyperbola between the two inferred end members, shown as coloured boxes.

As the formation of secondary soil phases such as clays or oxides exerts a strong control on the isotope signature of Li and Mg in the Mackenzie Basin (Millot et al., 2010; Tipper et al., 2012), it could be expected that such processes affect river dissolved Ba abundance and isotope composition. Nonetheless, the estimated fractionation factor for secondary phase formation is relatively low ($\Delta_{diss-solid}$ = 0.007 to 0.13‰; Gong et al., 2019), such that this process can hardly account for the observed high dissolved $\delta^{138}Ba_{diss}$ values in the Mackenzie Basin (around 0.40‰). Only the tributaries presenting the lowest $\delta^{138}Ba_{diss}$ values (Interior Platform, Fig. 4) are compatible with the fractionation expected for secondary phase formation. This is consistent with previous findings based on boron isotopes (Lemarchand and Gaillardet, 2006) showing that scavenging of weathering-derived element in soils or aquifers by mineral surfaces can be a significant process in the context of the Interior Platform.

Biological uptake could entail isotope fractionation raising $\delta^{138}Ba_{diss}$ towards higher values for some tributaries ($\Delta_{diss-bio}$ = 0.25 to 0.75‰; Bullen and Chadwick, 2016). To date, such an influence of the biota on river Ba loads has been reported only for tropical environments (Charbonnier et al., 2020). Hence, we expect that the cold climate of the Mackenzie Basin poses a limit to the role of biological productivity on river dissolved Ba abundance and isotope composition there.

The typical range of sediment concentrations in the Mackenzie Basin tributaries is in principle high enough to enable a significant effect of sorption of river dissolved Ba onto the river sediments (Gou et al., 2019; Bridgestock et al., 2021b). Consistently, leaching experiments performed on river sediments of the Mackenzie have revealed the adsorption of Ba (Larkin et al., 2021; Dellinger et al., 2021). Nevertheless, Ba released by desorption should be characterized by higher Ba/Na ratios together with a lighter Ba isotope composition (Gou et al., 2019; Bridgestock et al., 2021b), which is opposite to the relationship observed.

As a consequence, we propose that the mixing of different lithological weathering sources is the major driver of the relationship between Ba abundance and isotope composition in the Mackenzie Basin (Fig. 4). However, it is important to understand that processes can still act to define the composition of the dissolved mixing end members themselves.

On the one hand, we note that for most Mackenzie tributaries the dissolved Ba/Na* ratio - which is mostly influenced by silicate weathering, given the quasi-absence of Ba and Na in carbonate rocks - is lower than the range defined for sedimentary rocks, which represent the largest fraction of the Mackenzie Basin lithology (Millot et al., 2003; Dellinger et al., 2014). The depletion of Ba in rivers with respect to silicate rocks (Fig. 4) suggests that Ba is released incongruently with respect to Na, and/or that Ba released from silicate weathering is scavenged by processes after its release by mineral dissolution. As explained above, such depletion should be accompanied by Ba isotope fractionation. Consequently, the low-$(Ba/Na^*)_{diss}$, low-$\delta^{138}Ba_{diss}$ end member (yellow rectangle in Fig. 4), reflective of Mackenzie tributaries draining the Interior Platform, is most likely resulting from Ba scavenging by sorption onto particles or secondary phase formation after silicate rock dissolution, shifting the composition of the silicate rock dissolution end member towards lower Ba/Na ratios and higher $\delta^{138}Ba$ values (grey arrows in Fig. 4).

On the other hand, the high-$(Ba/Na^*)_{diss}$ and $\delta^{138}Ba_{diss}$ end member (red rectangle in Fig. 4) requires the contribution of a Ba-rich rock source with a heavy Ba isotope signature (> 0.40‰), that would be particularly prominent in the Rocky mountains and for some of the main tributaries (Red Arctic, Liard and Peel). Again, it is possible that the composition of this dissolved end member, inferred by the trend between $(Ba/Na^*)_{diss}$ and $\delta^{138}Ba_{diss}$, is different from that of the source rock composition itself, due to some secondary processes affecting the rock dissolution.

Therefore, we propose that the overall offset in Ba/Na* ratio and $\delta^{138}Ba$ values between the dissolved load and typical siliciclastic rocks is likely to derive from sorption onto solids, either in soils or in rivers, or secondary phase formation. Of course, such secondary processes might influence dissolved Ba abundance and isotope composition to a different extent in each river, but the strong relationship observed in Fig. 4 suggests a limited variation of the extent of Ba scavenging across the Mackenzie Basin. Therefore, our findings emphasise the role of source mixing as the main driver of the relationship between dissolved Ba and its isotopes across the Mackenzie Basin, as inferred from the examination of sediment data in Section 4.1. In particular, this mixing explanation requires the existence of an isotopically-heavy Ba source, for which we discuss potential candidates in the next section.

#### 4.2.2. *Black shale weathering as a source of heavy Ba in the Mackenzie River*

In an attempt to identify the source of heavy Ba in river of the Mackenzie Basin, we first examine the relationship between $\delta^{138}Ba_{diss}$ and $(^{87}Sr/^{86}Sr)_{diss}$. Indeed, "radiogenic" $^{87}Sr/^{86}Sr$ ratios are not fractionated by weathering processes and therefore are particularly useful for discriminating the relative contribution of various lithological sources (e.g., Palmer and Edmond, 1992).

The positive trend displayed in Fig. 5a between $\delta^{138}Ba_{diss}$ and $(^{87}Sr/^{86}Sr)_{diss}$ is indicative of a lithological control on the abundance and isotope composition of dissolved Ba in the Mackenzie Basin. This trend further suggests that the source of heavy Ba isotope is not associated with the weathering of igneous rocks (expected to be characterized by relatively low $^{87}Sr/^{86}Sr$ ratios; Gaillardet et al., 1999). Higher $\delta^{138}Ba_{diss}$ values are in fact associated with more radiogenic Sr signatures (Fig. 5a), suggesting that the source of heavy Ba are old sedimentary silicate rocks, as inferred in Section 4.1 from the composition of river sediments. However, the available data on siliciclastic rocks does not show significantly different Ba isotope composition compared to typical UCC rocks (Nan et al., 2018; Charbonnier et al., 2020). In that respect, we note that the $\delta^{138}Ba$ values of fine river suspended sediments in the Mackenzie Basin are indistinguishable from the siliciclastic rocks. Therefore, the trend of Fig. 5a suggests that the source of heavy Ba isotope in the Mackenzie river dissolved load is not the weathering of silicate sedimentary rocks itself, but derives from the weathering and erosion of a specific phase (possibly several specific phases) within the same sedimentary units. As a consequence, the river dissolved Sr isotope composition indicates that the source of heavy Ba in the Mackenzie Basin is most likely old siliciclastic rocks.

Interestingly, the rivers with higher $^{87}Sr/^{86}Sr$ and $\delta^{138}Ba_{diss}$ (such as the Racing, Toad, Peel, and Red Arctic) are tributaries for which black shales are thought to have a major influence on the river chemistry. The positive relationships observed between $\delta^{138}Ba_{diss}$ on the one hand and the dissolved $SO_{4pyr}/Na^*$ (a proxy for sulphide-derived river dissolved sulphate; Calmels et al., 2007) and $^{187}Os/^{188}Os$ ratios (a proxy for black shale weathering; Huh et al., 2004; Georg et al., 2013) on the other hand (Fig. 5b,c) show that the high $\delta^{138}Ba_{diss}$ of the Rocky Mountain regions are associated with black shale weathering, in line with inferences based

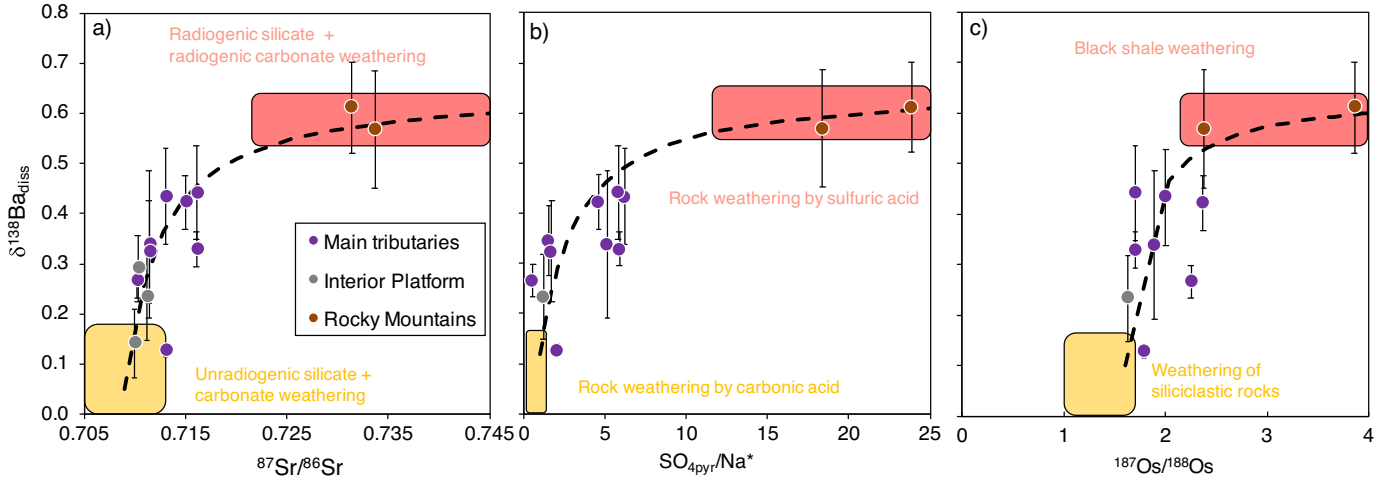


**Fig. 5.** Dissolved $\delta^{138}Ba$ values *vs.* (a) $^{87}Sr/^{86}Sr$ ratios; (b) $SO_{4\ pyr}/Na^*$ ratios, where $SO_{4\ pyr}$ refers to the concentration of river dissolved $SO_4^{2-}$ deriving from sulphide oxidation only (as constrained by Calmels et al., 2007); (c) $^{187}Os/^{188}Os$ ratios, where high $^{187}Os/^{188}Os$ ratios are associated with Os release from black shale weathering and low $^{187}Os/^{188}Os$ ratios are associated with the release of dissolved Os from the weathering of other types of silicate rock. The stippled curve corresponds to a mixing hyperbola between the two inferred end members, represented as coloured boxes.

on the composition of river sediments (Section 4.1).

As for the weathering of other types of siliciclastic rocks, the range of Ba/Na ratio for black shales is much higher than for the Mackenzie dissolved load (*e.g.*, $(Ba/Na)_{blackshale} \sim 1$, while the highest $(Ba/Na^*)_{diss}$ of the Mackenzie is around 0.03; Fig. 4; Fraser and Hutchison, 2017), suggesting that Ba released from black shale weathering is also affected by processes such as sorption or secondary phase formation (Gou et al., 2019; Gong et al., 2019; Bridgestock et al., 2021b). Despite such strong depletion in dissolved Ba abundance compared to the source rock, the heaviest $\delta^{138}Ba_{diss}$ is higher by only ~ 0.2‰ compared to the heaviest $\delta^{138}Ba_{sed}$. This again suggests that secondary weathering processes have a limited influence on Ba isotopes in the Mackenzie River, although their influence on Ba abundance cannot be dismissed.

The exact reason for black shale weathering producing such high $\delta^{138}Ba_{diss}$ and Ba concentration values (Fig. 4) remains relatively elusive. Only one $\delta^{138}$Ba value has been reported for black shale rocks (Tian et al., 2020), which is insufficient to ascertain a pervasive heavy $\delta^{138}$Ba signature for black shale. Alternatively, a broad range of $\delta^{138}$Ba for water reservoirs associated with (and potentially trapped within) black shale formations has been reported by Tieman et al. (2020). Nonetheless, we acknowledge that significant differences exist between our study and that of Tieman et al. (2020) as: 1) the waters analyzed by Tieman et al. (2020) derive from rock fracking in the context of shale gas extraction; and 2) the Marcellus shale formation studied by Tieman et al. (2020) is not reported to be present in the Rocky Mountains. Consequently, in the next section, we seek to discuss which reasons could lead to the heavy $\delta^{138}$Ba signature found in the black shales of the Mackenzie Basin.

### 4.3. What is the origin of the Ba-rich, heavy-Ba component released by black shale weathering?

Black shales usually consist in a complex assembly of different mineralogical phases (*e.g.*, Fraser and Hutchison, 2017). Several of these phases are unlikely to host significant amounts of Ba. As explained above, carbonate minerals usually associated with black shale formations are not known to contain significant amounts of Ba (Dehairs et al., 1980). In addition, leaching experiments and sequential extractions performed on Mackenzie river sediments (Larkin et al., 2021; Dellinger et al., 2021) reveal that Ba is mostly hosted in phases only digested by Aqua Regia and HF - thus ruling out the role of carbonate or other readily-dissolved phases as major Ba hosting phases.

Given the low affinity of Ba for -II-valence anions, sulphide are thought to be poor in Ba. The abundance of Ba in organic-poor shales does not differ from that of igneous rocks (Rudnick and Gao, 2003), suggesting that the clay component of black shales is not the most likely candidate for a Ba-rich reservoir. In addition, the clay-rich (high Li/Al ratio) component of the Mackenzie Basin river sediments displays low $\delta^{138}$Ba values (Fig. 3), which makes the clay mineral component of black shales an unlikely contributor to their heavy Ba signature. The organic matter present in black shales could in principle contain significant amounts of Ba, as suggested by the positive relationship between dissolved Os isotope ratios and Ba isotope composition (Fig. 5c). The elevated sediment Ba abundance observed for some rivers in the Mackenzie River (around 1000–1500 mg/kg; Table 2) can hardly be explained by the Ba content usually measured in fresh organic matter (Li, 2000) - although we acknowledge that Ba abundance in oceanic organic matter could increase during diagenesis, a yet-unquantified effect. As a consequence, the elevated sediment Ba abundance measured for some tributaries of the Mackenzie can only be reached through the contribution of "pure" Ba-bearing phases. The partial dissolution of these phases would then results in the heavy dissolved Ba signatures observed in river waters (Fig. 4).

Therefore, a possible candidate for this Ba-rich mineralogical component present in marine sedimentary rocks, especially in black shales, is barite. Black shale formations can indeed be associated with barite layers (Fraser and Hutchison, 2017). However, two observations challenge this interpretation.

First, the river sediment Ba/Al ratio (which can be used as a proxy for the abundance of barite *vs.* silicate minerals in sediments; Bridgestock et al., 2018) does not show any positive relation with sediment $\delta^{138}$Ba values (Fig. 3c). For example, the Toad and Racing rivers show the highest contribution from black shale weathering (high dissolved Os signature and $SO_{4pyr}/Na^*$; Fig. 5) and the highest dissolved Ba/Na* ratios and $\delta^{138}$Ba values (Fig. 4), whereas their sediments do not show significant Ba excess compared to typical crustal rocks (less than 800 mg/kg; Table 2). However, we note that rivers draining the Rocky Mountains are typically exporting solids and dissolved matter that are not "in equilibrium", meaning that they do not reflect weathering processes over the same time scales (Vigier et al., 2001). For example, a recent change in erosion rate should typically entail a modification in weathering rates, but such modification could take some time, possibly resulting in changes in sediment fluxes but not yet in solute fluxes.

Second, a compilation of marine barite $\delta^{138}$Ba values results in an average Ba isotope composition of 0.00‰ (Crockford et al., 2019), which does not offer an explanation for the high $\delta^{138}$Ba values observed in this study (around 0.20‰ in average). However, it could first be hypothesized that the black shale formations underlying the Mackenzie Basin host high-$\delta^{138}$Ba barite, with values outside of the range reported by Crockford et al. (2019), *e.g.* due to different depositional age (hence different Ba isotope composition of seawater) or to post-depositional processes. This would be needed to explain the $\delta^{138}$Ba values of ~ 0.20–0.40‰ observed in some river sediments of the Mackenzie Basin (this study) and for muds extracted from the Marcellus shale formation (Tieman et al., 2020). Alternatively, fractionating processes during (or following) barite dissolution could account for the high $\delta^{138}Ba_{diss}$ values (~ 0.80–1.00‰) observed in the Mackenzie Basin and in waters extracted from the Marcellus shale formation (Tieman et al., 2020).

Clearly, more research is needed to pinpoint the exact mineralogical sources and chemical processes that can account for the observed heavy $\delta^{138}$Ba values in river materials of the Mackenzie Basin. However, in any case our findings challenge the common assumption previously made that weathering of "classical" silicate rocks is the only source of river dissolved Ba (Bullen and Chadwick, 2016; Gong et al., 2019; Gou et al., 2019; Charbonnier et al., 2020). Our analysis emphasises how Ba sourced from black shale weathering can display a specific $\delta^{138}$Ba signature and thus may affect the Earth surface Ba isotope cycle. In particular, although the river Ba flux downstream from estuaries is thought to have an isotope composition close to that of the UCC (Bridgestock et al., 2021b), an enhanced contribution of black shale weathering having a distinct isotope signature might be able to shift the dissolved Ba flux to the ocean, that can in turn affect the isotope signature recorded in sedimentary archives. Such effect could obscure potential past changes in ocean Ba isotope composition due to shifts in palaeo-productivity alone.

## 5. Conclusion

The $\delta^{138}$Ba values of river material in the Mackenzie Basin (ranging from 0.13 to 0.61‰ for the dissolved load, and from −0.02 to 0.35‰ for the solid load) span a much higher range than reported in previous work (Cao et al., 2016; Gong et al., 2019; Gou et al., 2019; Charbonnier et al., 2020; Bridgestock et al., 2021a, 2021b).

In river sediments, the highest $\delta^{138}$Ba are found in river bed sediments deriving preferentially from the erosion of black shales. In the dissolved load, $\delta^{138}$Ba values result from a binary mixing between two distinct weathering sources. The first end member, characterized by low Ba abundance and light Ba isotope composition corresponds to Ba inputs from the weathering of igneous and siliciclastic rocks. We note that the composition of this end member is not strictly the composition of the source silicate minerals, but is also most likely partly controlled by secondary phase formation and/or adsorption onto river or soil

particles. The second weathering end member, enriched in Ba and in particular in heavy Ba isotopes, and sourced from weathering in the Rocky Mountains, is more difficult to constrain. We suggest that it corresponds to black shale weathering based on relationships between Ba elemental and isotope signatures and the "radiogenic" isotope systems of Sr and Os.

Altogether, our study emphasises the significant supply of Ba from black shale weathering at the scale of a large river catchment. Although previous findings have suggested the role of processes in setting the Ba isotope composition in the weathering environment, the weathering of black shale is able to deliver a dissolved Ba isotope signature that is different from that of the weathering of other silicate rocks. Consequently, addressing the modern as well as past riverine Ba flux to the ocean requires to take into account the black shale as a prominent supply of Ba to rivers.

Supplementary data to this article can be found online at https://doi.org/10.1016/j.chemgeo.2022.120741.

## Declaration of Competing Interest

The authors declare that they have no known competing financial interests or personal relationships that could have appeared to influence the work reported in this paper.

## Acknowledgements

The authors are grateful to Pascale Louvat, Jessica Dallas, Thibaud Sontag, and Laëticia Faure for analytical support. The manuscript greatly benefited from insightful discussions with Bob Hilton, Albert Galy and Frédéric Moynier. Luke Bridgestock and an anonymous reviewer are thanked for their constructive comments that improved the paper. Christian France-Lanord is thanked for editorial handling of the paper. Geochemical analyses presented in this study were enabled by the IPGP multidisciplinary program PARI and by the Region Île-de-France SESAME Grant no. 12015908, and by the grant "Émergences" awarded by the city of Paris awarded to Julien Bouchez.

## References

Bates, S.L., Hendry, K.R., Pryer, H.V., Kinsley, C.W., Pyle, K.M., Woodward, E.M.S., Horner, T.J., 2017. Barium isotopes reveal role of ocean circulation on barium cycling in the Atlantic. Geochim. Cosmochim. Acta 204, 286–299.
Bouchez, J., Gaillardet, J., France-Lanord, C., Maurice, L., Dutra-Maia, P., 2011. Grain size control of river suspended sediment geochemistry: Clues from Amazon River depth profiles. Geochem. Geophys. Geosyst. 12 (3).
Bridgestock, L., Hsieh, Y.-T., Porcelli, D., Homoky, W.B., Bryan, A., Henderson, G.M., 2018. Controls on the barium isotope compositions of marine sediments. Earth Planet. Sci. Lett. 481, 101–110.
Bridgestock, L., Hsieh, Y.-T., Porcelli, D., Henderson, G.M., 2019. Increased export production during recovery from the Paleocene–Eocene thermal maximum constrained by sedimentary Ba isotopes. Earth Planet. Sci. Lett. 510, 53–63.
Bridgestock, L., Nathan, J., Hsieh, Y.-T., Holdship, P., Porcelli, D., Andersson, P.S., Henderson, G.M., 2021a. Assessing the utility of barium isotopes to trace eurasian riverine freshwater inputs to the arctic ocean. Mar. Chem. 236, 104029.
Bridgestock, L., Nathan, J., Paver, R., Hsieh, Y.-T., Porcelli, D., Tanzil, J., Holdship, P., Carrasco, G., Annammala, K.V., Swarzenski, P.W., et al., 2021b. Estuarine processes modify the isotope composition of dissolved riverine barium fluxes to the ocean. Chem. Geol. 579, 120340.
Bullen, T., Chadwick, O., 2016. Ca, Sr and Ba stable isotopes reveal the fate of soil nutrients along a tropical climosequence in Hawaii. Chem. Geol. 422, 25–45.
Calmels, D., Gaillardet, J., Brenot, A., France-Lanord, C., 2007. Sustained sulfide oxidation by physical erosion processes in the Mackenzie River Basin: climatic perspectives. Geology 35 (11), 1003–1006.
Cao, Z., Siebert, C., Hathorne, E.C., Dai, M., Frank, M., 2016. Constraining the oceanic barium cycle with stable barium isotopes. Earth Planet. Sci. Lett. 434, 1–9.
Cao, Z., Siebert, C., Hathorne, E.C., Dai, M., Frank, M., 2020. Corrigendum to" constraining the oceanic barium cycle with stable barium isotopes"[earth planet. Sci. Lett. 434 (2016) 1-9]. E&PSL 530, 116003.
Cao, Z., Rao, X., Yu, Y., Siebert, C., Hathorne, E.C., Liu, B., Wang, G., Lian, E., Wang, Z., Zhang, R., et al., 2021. Stable barium isotope dynamics during estuarine mixing. Geophys. Res. Lett. 48 (19), e2021GL095680.
Carson, M., Jasper, J., Conly, F.M., 1998. Magnitude and sources of sediment input to the Mackenzie Delta, Northwest Territories, 1974–94. Arctic 116–124.
Charbonnier, Q., Moynier, F., Bouchez, J., 2018. Barium isotope cosmochemistry and geochemistry. Sci. Bull. 63 (6), 385–394.
Charbonnier, Q., Bouchez, J., Gaillardet, J., Gayer, É., 2020. Barium stable isotopes as a fingerprint of biological cycling in the Amazon River basin. Biogeosciences 17 (23), 5989–6015.
Coffey, M., Dehairs, F., Collette, O., Luther, G., Church, T., Jickells, T., 1997. The behaviour of dissolved barium in estuaries. Estuar. Coast. Shelf Sci. 45 (1), 113–121.
Cooper, L., McClelland, J., Holmes, R., Raymond, P., Gibson, J., Guay, C., Peterson, B., 2008. Flow-weighted values of runoff tracers ($\delta^{18}$O, DOC, Ba, alkalinity) from the six largest arctic rivers. Geophys. Res. Lett. 35 (18).
Crockford, P.W., Wing, B.A., Paytan, A., Hodgskiss, M.S., Mayfield, K.K., Hayles, J.A., Middleton, J.E., Ahm, A.-S.C., Johnston, D.T., Caxito, F., et al., 2019. Barium-isotopic constraints on the origin of post-marinoan barites. Earth Planet. Sci. Lett. 519, 234–244.
Dalai, T.K., Krishnaswami, S., Sarin, M.M., 2002a. Barium in the Yamuna River system in the Himalaya: sources, fluxes, and its behavior during weathering and transport. Geochem. Geophys. Geosyst. 3 (12), 1–23.
Dalai, T.K., Singh, S.K., Trivedi, J., Krishnaswami, S., 2002b. Dissolved rhenium in the Yamuna River System and the Ganga in the Himalaya: Role of black shale weathering on the budgets of Re, Os, and U in rivers and $CO_2$ in the atmosphere. Geochim. Cosmochim. Acta 66 (1), 29–43.
Dehairs, F., Chesselet, R., Jedwab, J., 1980. Discrete suspended particles of barite and the barium cycle in the open ocean. Earth Planet. Sci. Lett. 49 (2), 528–550.
Dellinger, M., Gaillardet, J., Bouchez, J., Calmels, D., Galy, V., Hilton, R.G., Louvat, P., France-Lanord, C., 2014. Lithium isotopes in large rivers reveal the cannibalistic nature of modern continental weathering and erosion. Earth Planet. Sci. Lett. 401, 359–372.
Dellinger, M., Hilton, R.G., Nowell, G.M., 2021. Fractionation of rhenium isotopes in the Mackenzie River basin during oxidative weathering. Earth Planet. Sci. Lett. 573, 117131.
Fraser, T.A., Hutchison, M.P., 2017. Lithogeochemical characterization of the middle–upper devonian road river group and canol and imperial formations on trail river, East Richardson mountains, Yukon: age constraints and a depositional model for fine-grained strata in the lower paleozoic Richardson trough. Can. J. Earth Sci. 54 (7), 731–765.
Gaillardet, J., Dupré, B., Louvat, P., Allègre, C.J., 1999. Global silicate weathering and $CO_2$ consumption rates deduced from the chemistry of large rivers. Chem. Geol. 159 (1–4), 3–30.
Gaillardet, J., Millot, R., Dupré, B., 2003. Chemical denudation rates of the western Canadian orogenic belt: the Stikine terrane. Chem. Geol. 201 (3–4), 257–279.
Gaillardet, J., Viers, J., Dupré, B., 2014. Trace elements in river waters. Treat. Geochem. 5, 605.
Georg, R.B., West, A.J., Vance, D., Newman, K., Halliday, A., 2013. Is the marine osmium isotope record a probe for $CO_2$ release from sedimentary rocks? Earth Planet. Sci. Lett. 367, 28–38.
Gong, Y., Zeng, Z., Zhou, C., Nan, X., Yu, H., Lu, Y., Li, W., Gou, W., Cheng, W., Huang, F., 2019. Barium isotopic fractionation in latosol developed from strongly weathered basalt. Sci. Total Environ. 687, 1295–1304.
Gou, L.-F., Jin, Z., Galy, A., Gong, Y.-Z., Nan, X.-Y., Jin, C., Wang, X.-D., Bouchez, J., Cai, H.-M., Chen, J.-B., et al., 2019. Seasonal riverine barium isotopic variation in the middle yellow river: Sources and fractionation. Earth Planet. Sci. Lett. 115990.
Gower, C.F., Schärer, U., Heaman, L.M., 1992. The Labradorian orogeny in the Grenville province, eastern Labrador, Canada. Can. J. Earth Sci. 29 (9), 1944–1957.
Guay, C., Falkner, K.K., 1998. A survey of dissolved barium in the estuaries of major arctic rivers and adjacent seas. Cont. Shelf Res. 18 (8), 859–882.
Hilton, R.G., Galy, V., Gaillardet, J., Dellinger, M., Bryant, C., O'regan, M., Gröcke, D.R., Coxall, H., Bouchez, J., Calmels, D., 2015. Erosion of organic carbon in the Arctic as a geological carbon dioxide sink. Nature 524 (7563), 84.
Holmes, R.M., McClelland, J.W., Peterson, B.J., Shiklomanov, I.A., Shiklomanov, A.I., Zhulidov, A.V., Gordeev, V.V., Bobrovitskaya, N.N., 2002. A circumpolar perspective on fluvial sediment flux to the arctic ocean. Glob. Biogeochem. Cycles 16 (4), 45–1.
Horan, K., Hilton, R., Dellinger, M., Tipper, E., Galy, V., Calmels, D., Selby, D., Gaillardet, J., Ottley, C., Parsons, D., et al., 2019. Carbon dioxide emissions by rock organic carbon oxidation and the net geochemical carbon budget of the Mackenzie River Basin. Am. J. Sci. 319 (6), 473–499.
Horner, T.J., Kinsley, C.W., Nielsen, S.G., 2015. Barium-isotopic fractionation in seawater mediated by barite cycling and oceanic circulation. Earth Planet. Sci. Lett. 430, 511–522.
Hsieh, Y.-T., Henderson, G.M., 2017. Barium stable isotopes in the global ocean: Tracer of Ba inputs and utilization. Earth Planet. Sci. Lett. 473, 269–278.
Huh, Y., Birck, J.-L., Allègre, C.J., 2004. Osmium isotope geochemistry in the Mackenzie River Basin. Earth Planet. Sci. Lett. 222 (1), 115–129.
Larkin, C.S., Piotrowski, A.M., Hindshaw, R.S., Bayon, G., Hilton, R.G., Baronas, J.J., Dellinger, M., Wang, R., Tipper, E.T., 2021. Constraints on the source of reactive phases in sediment from a major arctic river using neodymium isotopes. Earth Planet. Sci. Lett. 565, 116933.
Lemarchand, D., Gaillardet, J., 2006. Transient features of the erosion of shales in the Mackenzie Basin (Canada), evidences from boron isotopes. Earth Planet. Sci. Lett. 245 (1–2), 174–189.
Li, Y.H., 2000. A Compendium of Geochemistry: From Solar Nebula to the Human Brain. Princeton University Press.
Millot, R., Gaillardet, J., Dupré, B., Allègre, C.J., 2002. The global control of silicate weathering rates and the coupling with physical erosion: new insights from rivers of the Canadian Shield. Earth Planet. Sci. Lett. 196 (1–2), 83–98.

Millot, R., Gaillardet, J., Dupré, B., Allègre, C.J., 2003. Northern latitude chemical weathering rates: clues from the Mackenzie River Basin, Canada. Geochim. Cosmochim. Acta 67 (7), 1305–1329.
Millot, R., Vigier, N., Gaillardet, J., 2010. Behaviour of lithium and its isotopes during weathering in the Mackenzie Basin, Canada. Geochim. Cosmochim. Acta 74 (14), 3897–3912.
Nan, X.-Y., Yu, H.-M., Rudnick, R.L., Gaschnig, R.M., Xu, J., Li, W.-Y., Zhang, Q., Jin, Z.-D., Li, X.-H., Huang, F., 2018. Barium isotopic composition of the Upper Continental Crust. Geochim. Cosmochim. Acta 233, 33–49.
Palmer, M.R., Edmond, J.M., 1992. Controls over the strontium isotope composition of river water. Geochim. Cosmochim. Acta 56 (5), 2099–2111.
Paytan, A., Griffith, E.M., 2007. Marine barite: Recorder of variations in ocean export productivity. Deep-Sea Res. II Top. Stud. Oceanogr. 54 (5), 687–705.
Reeder, S., Hitchon, B., Levinson, A., 1972. Hydrogeochemistry of the surface waters of the Mackenzie River drainage basin, Canada. Factors controlling inorganic composition. Geochim. Cosmochim. Acta 36 (8), 825–865.
Rudnick, R.L., Gao, S., 2003. Composition of the Continental Crust. Treat. Geochem. 3, 659.
Samanta, S., Dalai, T.K., 2016. Dissolved and particulate barium in the ganga (hooghly) river estuary, India: Solute-particle interactions and the enhanced dissolved flux to the oceans. Geochim. Cosmochim. Acta 195, 1–28.
Taylor, S.R., McLennan, S.M., 1995. The geochemical evolution of the continental crust. Rev. Geophys. 33 (2), 241–265.
Tian, L.-L., Gong, Y.-Z., Wei, W., Kang, J.-T., Yu, H.-M., Huang, F., 2020. Rapid determination of Ba isotope compositions for barites using $H_2O$-extraction method and MC-ICP-MS. J. Anal. At. Spectrom. 35 (8), 1566–1573.
Tieman, Z.G., Stewart, B.W., Capo, R.C., Phan, T., Lopano, C., Hakala, J.A., 2020. Barium isotopes track the source of dissolved solids in produced water from the unconventional Marcellus Shale Gas Play. Environ. Sci. Technol. 54 (7), 4275–4285.
Tipper, E.T., Calmels, D., Gaillardet, J., Louvat, P., Capmas, F., Dubacq, B., 2012. Positive correlation between Li and Mg isotope ratios in the river waters of the Mackenzie Basin challenges the interpretation of apparent isotopic fractionation during weathering. Earth Planet. Sci. Lett. 333, 35–45.
Van Zuilen, K., Nägler, T.F., Bullen, T.D., 2016. Barium isotopic compositions of geological reference materials. Geostand. Geoanal. Res. 40 (4), 543–558.
Vigier, N., Bourdon, B., Turner, S., Allègre, C.J., 2001. Erosion timescales derived from u-decay series measurements in rivers. Earth Planet. Sci. Lett. 193 (3–4), 549–563.